



Published in final edited form as:

J Am Chem Soc. 2017 December 06; 139(48): 17301–17304. doi:10.1021/jacs.7b10639.

A rhodium-cyanine fluorescent probe: detection and signaling of mismatches in DNA

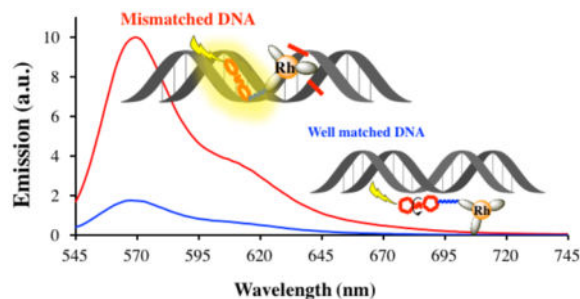
Adela Nano, Adam N. Boynton, and Jacqueline K. Barton*

California Institute of Technology, Division of Chemistry and Chemical Engineering, Pasadena, California 91125, United States

Abstract

We report a bifunctional fluorescent probe that combines a rhodium metalloinsertor with a cyanine dye as the fluorescent reporter. The conjugate shows weak luminescence when free in solution or with well matched DNA but exhibits a significant luminescence increase in the presence of a 27-mer DNA duplex containing a central CC mismatch. DNA photocleavage experiments demonstrate that, upon photoactivation, the conjugate cleaves the DNA backbone specifically near the mismatch site on a 27-mer fragment, consistent with mismatch targeting. Fluorescence titrations with the 27-mer duplex containing the CC mismatch reveal a DNA binding affinity of $3.1 \times 10^6 \text{ M}^{-1}$, similar to that of other rhodium metalloinsertors. Fluorescence titrations using genomic DNA extracted from various cell lines demonstrate a clear discrimination in fluorescence between those cell lines that are proficient or deficient in mismatch repair. This differential luminescence reflects the sensitive detection of the mismatch repair-deficient phenotype.

Graphical abstract



Within the cell, the mismatch repair (MMR) machinery is critical for maintaining genomic fidelity. Deficiencies in MMR result in the accumulation of base:base mismatches and predispose the cell to cancerous transformation.¹ Various rhodium complexes have been designed that target and bind single base pair mismatches with high specificity and selectivity.^{2,3} These rhodium compounds bear the sterically expansive 5,6-chrysenes diimine (*chrysi*) ligand, and preferentially target thermodynamically destabilized mismatches over

*Corresponding Author: jkbaron@caltech.edu.

Supporting Information

The Supporting Information is available free of charge on the ACS Publications website. Experimental methods and supporting Figures (S1–S16) (PDF)

matched base pairs by a factor of >1000 through metalloinsertion.^{4,5} In addition, these complexes target and inhibit growth in MMR-deficient versus MMR-proficient cancer cells with high selectivity.^{2,6} Considering the strong association of MMR deficiency and cancer, the development of early diagnostic tools for DNA mismatches and deficiencies in MMR would be invaluable.

We have recently reported a class of ruthenium metalloinsertors that serve as luminescent “light switches” for single base mismatches in dsDNA.⁷ Luminescent Pt(II) complexes have also been investigated as mismatch probes.⁸ The use of small organic fluorophores for site-specific targeting of DNA mismatches has been reported but still remains a challenging goal.⁹ Since the rhodium metalloinsertors do not display luminescence but nonetheless show remarkable mismatch selectivity, we have developed an alternative strategy for a luminescent metalloinsertor, equipping the rhodium complex with an organic fluorophore to serve as the optical reporter.

To achieve a fluorescent reporter of DNA mismatches, we have designed a bifunctional conjugate, **RhCy3**, in which mismatch targeting is performed by the rhodium metalloinsertor $[\text{Rh}(\text{phen})(\text{chrysi})(\text{dpa})]^{3+}$ (*chrysi* = 5,6-chrysene diimine; *DPA* = 2,2'-dipyridylamine) and the optical output by the cationic indole trimethine cyanine (Cy3) fluorophore through a “light-up” effect (Figure 1). The two components are covalently linked through a polyethylene glycol (PEG) linker, enhancing water solubility. Furthermore, indocarbocyanines are known to have (i) high chemical- and photo-stability, (ii) low toxicity and (iii) strong absorption in the visible range with a sharp increase in fluorescence when interacting with DNA.¹⁰ We rationalized that the conjugate would not bind tightly to well matched DNA, resulting in weak luminescence. However, in the presence of a mismatched DNA duplex, the conjugate would recognize the mismatched site and bind tightly to the duplex; with Cy3 bound rigidly against the DNA groove, constraining rotation of Cy3 around the polymethine chain, an increased fluorescence from Cy3 would result. Minor groove binding and DNA intercalation are binding modes that are both observed for cyanines. Binding to DNA from the minor groove side is found both for the parent cyanine¹⁰ and rhodium complex.⁵

Thus, we synthesized and fully characterized the bifunctional fluorescent probe **RhCy3** containing a flexible PEG linker in a multistep procedure shown partially in Scheme 1. A peptidic coupling performed between the primary amine **DPA-NH₂** and **Cy3-COOH** gave **DPA-Cy3** in 86% yield. The complexation of the latter with the rhodium precursor yielded the final probe in good yield. Model compounds $[\text{Rh}(\text{phen})(\text{chrysi})(\text{HDPA})]^{3+}$ and the **Cy3-linker** (Figure 1), serving as spectroscopic references, were also prepared. The detailed experimental protocols and full characterization of **RhCy3** and model compounds are reported in the Supporting Information.

Electronic absorption profiles of the conjugate and spectroscopic references were obtained in Tris buffer (5 mM Tris, 200 mM NaCl, pH = 7.4) at ambient temperature (see Table S1 and Figure S1). The UV-visible spectrum of **RhCy3** resembles the sum of the absorption profiles of each component (Figure S1). The photoexcitation ($\lambda_{\text{EX}} = 520 \text{ nm}$) of **RhCy3** free in Tris buffer yields a weak luminescence with a maximum emission centered at 570 nm

(Figure 2), slightly red-shifted compared to the spectroscopic reference **Cy3-linker**; RhCy3 is also weaker in intensity compared to the free dye as a result of static quenching by the Rh complex. Significantly, the emission of the Rh probe (1 μM) is enhanced 9-fold in the presence of a 27-mer dsDNA containing a central CC mismatch (MM DNA, 1 μM). For these studies we utilized the highly destabilized CC mismatch; the parent Rh complex binds 80% of all mismatches depending upon their thermodynamic destabilization.⁵ Little fluorescence intensity increase is observed in the presence of fully well-matched (WM) DNA (Figure 2). In addition, no mismatch-dependent luminescence is found for the **Cy3-linker** lacking the metalloinsertor unit (Figure S2). We also examined the emission intensity of **RhCy3** in the presence of bovine serum albumin (BSA) at different concentrations, and no significant luminescence intensity increase was observed up to 50 equivalents of BSA (data not shown).

Fluorescence titrations with increasing amounts of 27-mer dsDNA containing a CC mismatch also show a strong increase in emission intensity (Figure 3), while with WM duplex, a negligible fluorescence increase is seen. The data were fit to a one-site specific binding equation to obtain the binding affinity of **RhCy3**, $K_B(\text{CC}) = 3.1 \times 10^6 \text{ M}^{-1}$, to the mismatched DNA sequence. This value is consistent with the binding affinities for other metalloinsertors including **[Rh(phen)(chrysi)(HDP)]Cl₃**,¹¹ indicating that the tethered fluorophore does not significantly affect the specific DNA binding affinity of the final conjugate.

Time-resolved fluorescence was also utilized to provide insight into the interaction of the conjugate with DNA. Fluorescence decay measurements were performed as previously described and data are gathered in Table 1.¹² The fluorescence decay profile of **RhCy3** when free in solution yields a monoexponential function with an excited state lifetime of 111 ps. The fluorescence lifetime of **RhCy3** in the presence of DNA (WM or MM) follows a biexponential decay function. However, in the presence of WM DNA, there is only a 4% extra population and clearly one major contribution from a population with a lifetime 116 ps. This value is in good agreement with the decay found for the free **RhCy3** indicating that there is no significant interaction between the conjugate and WM DNA.¹³

In the presence of MM DNA, the decay curve is biexponential with two excited state lifetimes: a major contribution (85%) from a species with $\tau_1 = 91$ ps and a smaller population (15%) with a significantly longer lifetime, $\tau_2 = 308$ ps, corresponding to the DNA-bound **RhCy3**. Constraining the cyanine through DNA binding would be expected to yield this increase in lifetime.¹⁴

The specific mismatch targeting can also be evaluated through DNA photocleavage experiments, since many of the Rh metalloinsertors promote site-specific DNA cleavage with irradiation.⁴ Following photolysis (320–440 nm), autoradiography, shown in Figure 4, reveals specific photocleavage of the mismatched duplex at the mismatched site similarly to **[Rh(bpy)₂(chrysi)]³⁺** and no photocleavage in the presence of WM DNA. Additionally, the **Cy3-linker** lacking the metalloinsertor moiety shows no DNA damage.

The MMR machinery increases genome fidelity during the replication process, but if the MMR machinery is defective, mismatches accumulate over time.¹ We therefore tested whether our conjugate could distinguish any differences in mismatch frequency associated with MMR-proficient versus MMR-deficient phenotypes using genomic DNA (gDNA) extracted from different MMR-proficient and -deficient cell lines. In a prior investigation,¹⁵ a rhodium(III) metalloinsertor bearing a benzo[*a*]phenazine-5,6-quinone diimine ligand was incubated with gDNA extracts from various MMR-deficient and -proficient cell lines. Indeed, following photo-activation, enhanced photocleavage was observed for those samples containing DNA from the MMR-deficient cell lines. Based on microsatellite instability and mutation frequency studies, there is an increase up to 1000-fold in mismatches in MMR-deficient versus MMR-proficient cells.^{16,1a} Remarkably, **RhCy3** fluorescence titrations show a significant increase in fluorescence intensity in the presence of gDNA isolated from MMR-deficient cells (HCT116O, DU145, and SKOV3) compared to gDNA isolated from the MMR-proficient HCT116N cell line (Figure 5).^{17,18} Thus, we find the conjugate to be capable of differentiating the MMR-deficient versus MMR proficient phenotype, and the results obtained for **RhCy3** correlate well with the reported mutation rates for these cell lines.^{15,17,19} This differential fluorescence enhancement reflects the remarkably high mismatch specificity of rhodium metalloinsertors; in fact, luminescent Ru(II) light switch complexes⁷ do not exhibit comparable mismatch discrimination in genomic DNA samples.

Overall these results demonstrate the design and application of a Rh metalloinsertor-cyanine conjugate in targeting mismatched DNA sites with a luminescent reporter of specific binding. A remarkably high sensitivity of the metalloinsertor conjugate to the MMR-deficient phenotype is observed which points to the application of the conjugate as a new tool in the early diagnosis of mismatch-repair deficient cancers.

Supplementary Material

Refer to Web version on PubMed Central for supplementary material.

Acknowledgments

Funding Sources

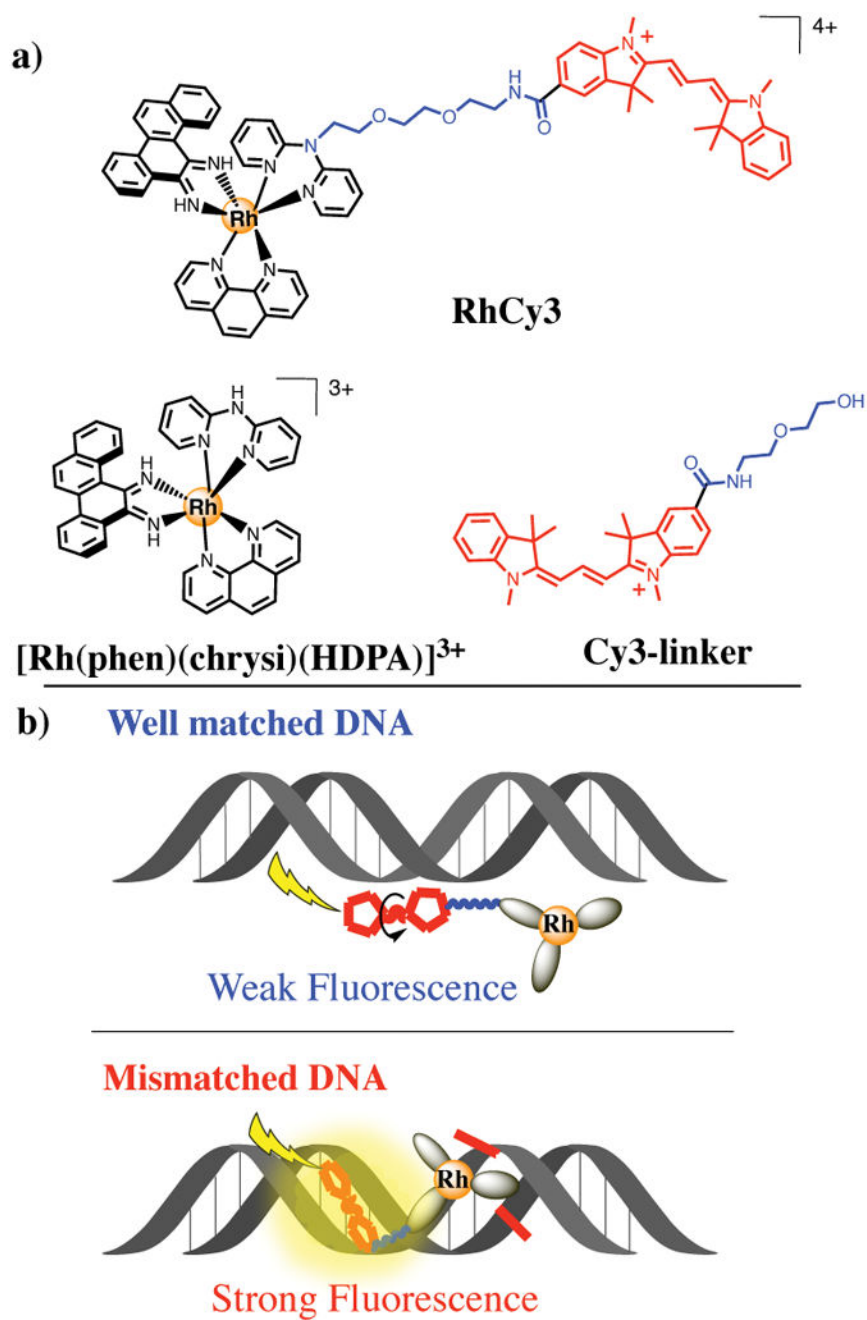
No competing financial interests have been declared.

We are grateful to the NIH for funding this work. We also thank the Beckman Institute Laser Resource Center facilities and Dr. Jay R. Winkler for assistance.

References

1. (a) Loeb LA. *Cancer Res.* 2001; 61:3230–3239. [PubMed: 11309271] (b) Bhattacharya NP, Skandalis A, Ganesh A, Groden J, Meuth M. *Proc Natl Acad Sci USA.* 1994; 91:6319–6323. [PubMed: 8022779] (c) Strauss BS. *Mutat Res.* 1999; 437:195–203. [PubMed: 10592327]
2. Zeglis BM, Pierre VC, Barton JK. *Chem Commun (Camb).* 2007; 44:4565–4579.
3. Komor AC, Barton JK. *J Am Chem Soc.* 2014; 136:14160–14172. [PubMed: 25254630]
4. Jackson BA, Alekseyev VY, Barton JK. *Biochemistry.* 1999; 38:4655–4662. [PubMed: 10200152]
5. Zeglis BM, Pierre VC, Kaiser JT, Barton JK. *Biochemistry.* 2009; 48:4247–4253. [PubMed: 19374348]

6. Hart JR, Golebov O, Ernst RJ, Kirsch IR, Barton JK. Proc Natl Acad Sci U S A. 2006; 103:15359–15363. [PubMed: 17030786]
7. (a) Boynton AN, Marcélis L, Barton JK. J Am Chem Soc. 2016; 138:5020–5023. [PubMed: 27068529] (b) Boynton AN, Marcélis L, McConnell AJ, Barton JK. Inorg Chem. 2017; 56:8381–8389. [PubMed: 28657712]
8. Fung SK, Zou T, Cao B, Chen T, To WP, Yang C, Lok CN, Che CM. Nat Commun. 2016; 7:1–9.
9. (a) Sato Y, Honjo A, Ishikawa D, Nishizawa S, Teramae N. Chem Commun. 2011; 47:5885–5887. (b) Arambula JF, Ramisetty SR, Baranger AM, Zimmerman SC. Proc Natl Acad Sci USA. 2009; 106:16068–16073. [PubMed: 19805260]
10. Cyanine's emissive properties strongly depend on the photo-induced *cis-trans* isomerization of the polymethine chain, which can be inhibited when cyanines are located in a rigid environment. See ref.: Levitus M, Ranjit S. Q Rev of Biophys. 2011; 44:123–151. [PubMed: 21108866]
11. Komor AC, Schneider CJ, Weidman AG, Barton JK. J Am Chem Soc. 2012; 123:19223–19233.
12. Messina MS, Axtell JC, Wang Y, Chong P, Wixtrom AI, Kirlikovali KO, Upton BM, Hunter BM, Shafaat OS, Khan SI, Winkler JR, Gray HB, Alexandrova AN, Maynard HD, Spokoyny AM. J Am Chem Soc. 2016; 138:6952–6955. [PubMed: 27186856]
13. Static quenching of the cyanine by the Rh complex is evident for the conjugate free in solution.
14. Harvey BJ, Levitus M. J Fluoresc. 2009; 19:443–448. [PubMed: 18972191]
15. Junicke H, Hart JR, Kisko J, Glebov O, Kirsch IR, Barton JK. Proc Natl Acad Sci U S A. 2003; 100:3737–3742. [PubMed: 12610209]
16. (a) Iyer RR, Pluciennik A, Burdett V, Modrich PI. Chem Rev. 2006; 106:302–323. [PubMed: 16464007] (b) Tomlinson I, Sasieni P, Bodmer W. Am J Path. 2002; 160:755–758. [PubMed: 11891172] (c) Koi M, Umar A, Chauhan DP, CherianSPCarethers JM, Kunkel TA, Boland CR. Cancer Res. 1994; 54:4308–4312. [PubMed: 8044777]
17. The fluorescence titrations with gDNA in conjunction with the data obtained from the fluorescence titrations with 27-*mer* dsDNA provide a lower estimate of the number of mismatches for MMR-deficient vs. MMR-proficient cells. Since the 27-*mer* DNA fluorescence titrations were performed with dsDNA containing only CC mismatches, we assume comparable or lower binding affinities to other (more thermodynamically stable) mismatches. Based on the fluorescence titrations with genomic samples, we therefore estimate about 500-fold increase in mismatches in cells that are MMR-deficient compared to the MMR-proficient analogue (SI, Section 8).
18. We also note that related metalloinsertors have been shown to bind abasic sites and single base bulges, which may be relevant to insertions and deletions that are similarly repaired by MMR machinery. See ref.: Zeglis BM, Boland JA, Barton JK. Biochemistry. 2009; 48:839–849. [PubMed: 19146409]
19. Glaab WE, Tindall KR. Carcinogenesis. 1997; 18:1–8. [PubMed: 9054582]

**Figure 1.**

a) Chemical structure of **RhCy3** and its spectroscopic references. b) Illustration of the interaction between the conjugate and DNA (well matched or mismatched).

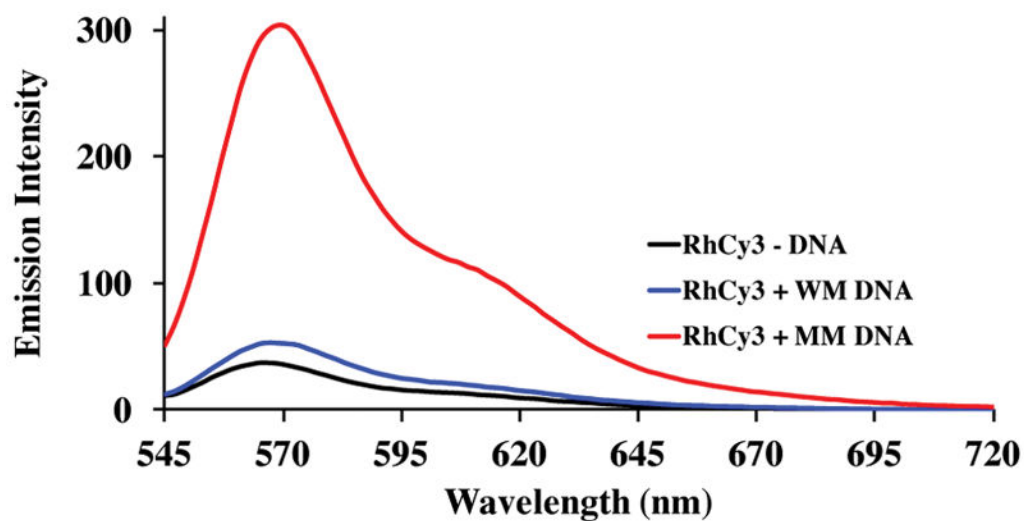


Figure 2. Steady-state emission spectra of **RhCy3** (1 μ M) free in solution (black), or in the presence of 1 μ M DNA duplex oligomer: WM DNA (blue) or MM DNA (red). The DNA duplex used was a 27-mer oligonucleotide with complement: 5'-GAC CAG CTT ATC ACC CCT AGA TAA GCG-3' where the MM strand contains a (C) at the mismatched site versus (G). In Tris buffer at 25 $^{\circ}$ C, $\lambda_{\text{Ex}} = 520$ nm.

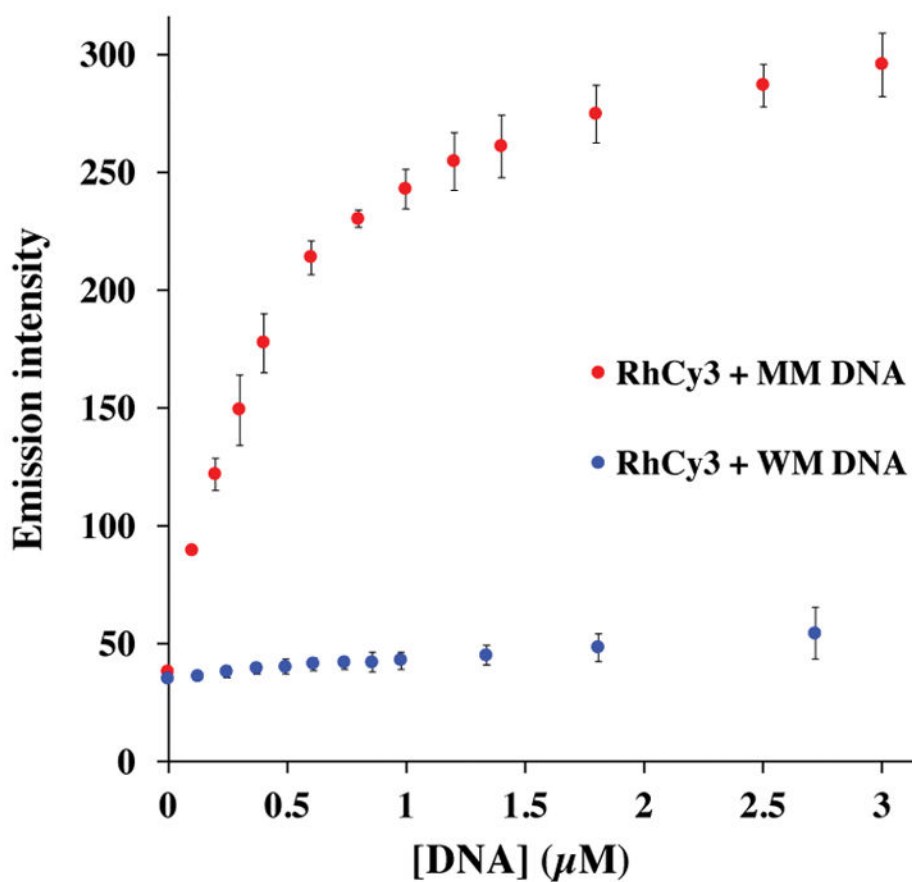


Figure 3. Fluorescence titrations with increasing amount of WM DNA (blue) and MM DNA (red). $[\text{RhCy3}] = 1 \mu\text{M}$, in Tris at 25°C . $\lambda_{\text{Ex}} = 520 \text{ nm}$. The 27-mer DNA sequence: $5' \text{-GAC CAG CTT ATC ACC CCT AGA TAA GCG-3'}$ where the MM strand comprises a (C) at the mismatched site versus (G) for WM. Error bars calculated over three replicates. [DNA] is per 27-mer sequence.

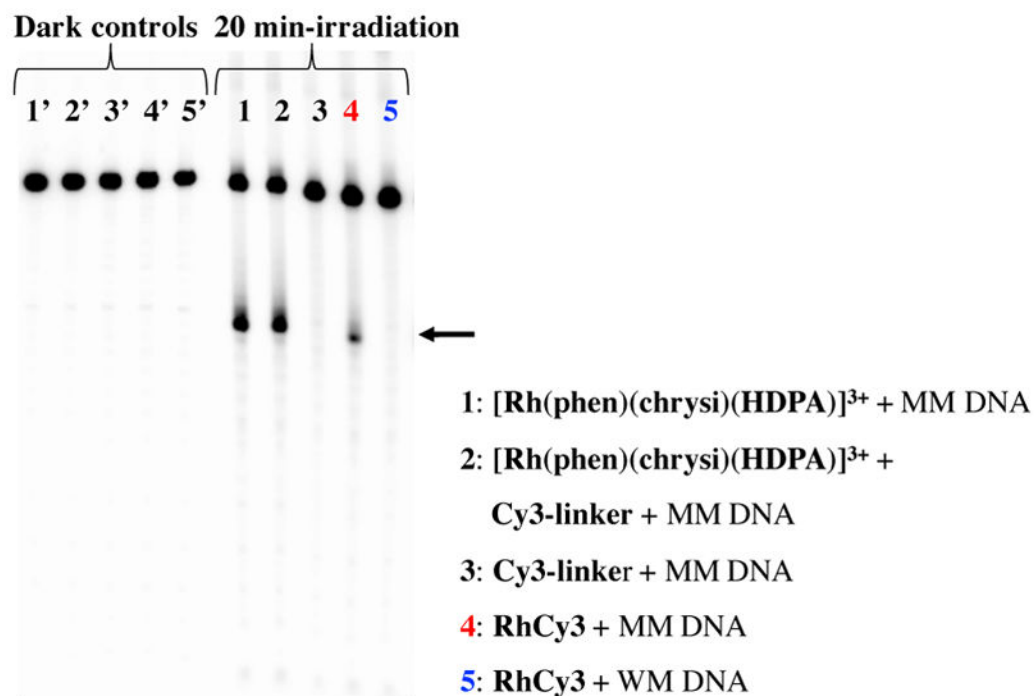


Figure 4.

Autoradiogram of a 20% polyacrylamide gel indicating photocleavage with MM DNA (lane 4). The dsDNA was a 27-mer 5'-³²P-GAC CAG CTT ATC ACC CCT AGA TAA GCG-3' where the MM strand comprises a (C) at the mismatched site versus (G) for the WM. The sample concentrations were 10 μ M in 20 mM NaCl, 10 mM NaPi, pH 7.1. Irradiations were carried out with a solar simulator (see SI). The arrow indicates the photocleaved DNA fragment nearby the mismatched site.

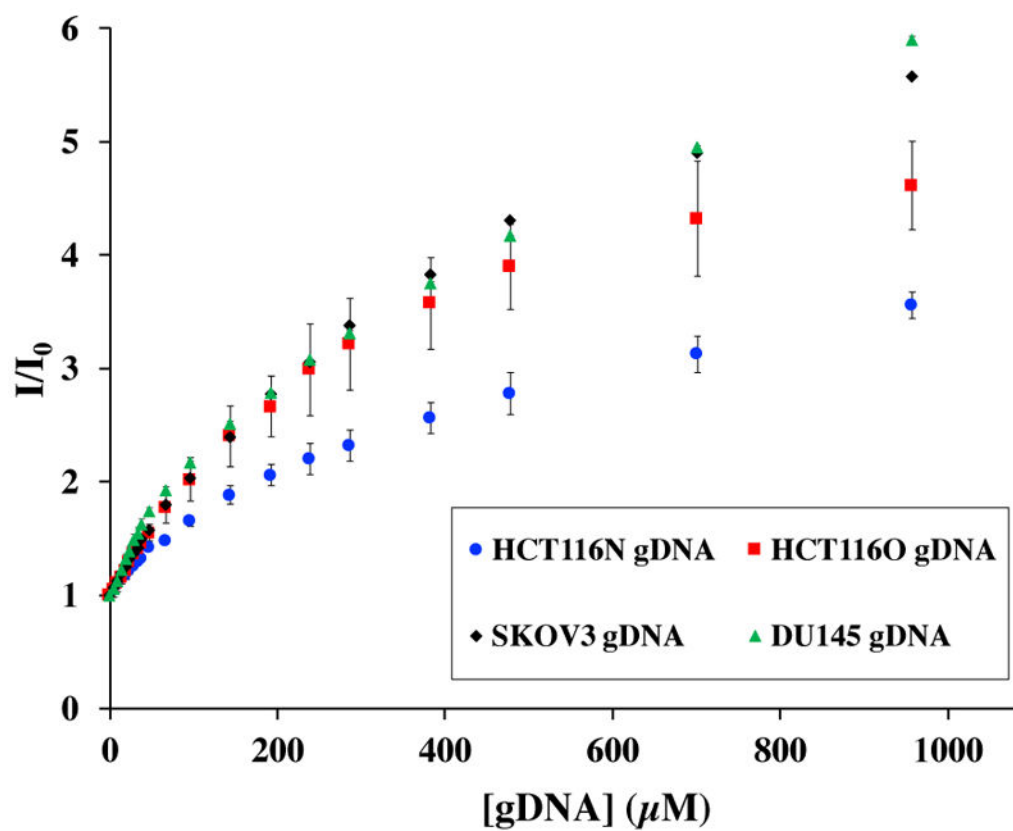
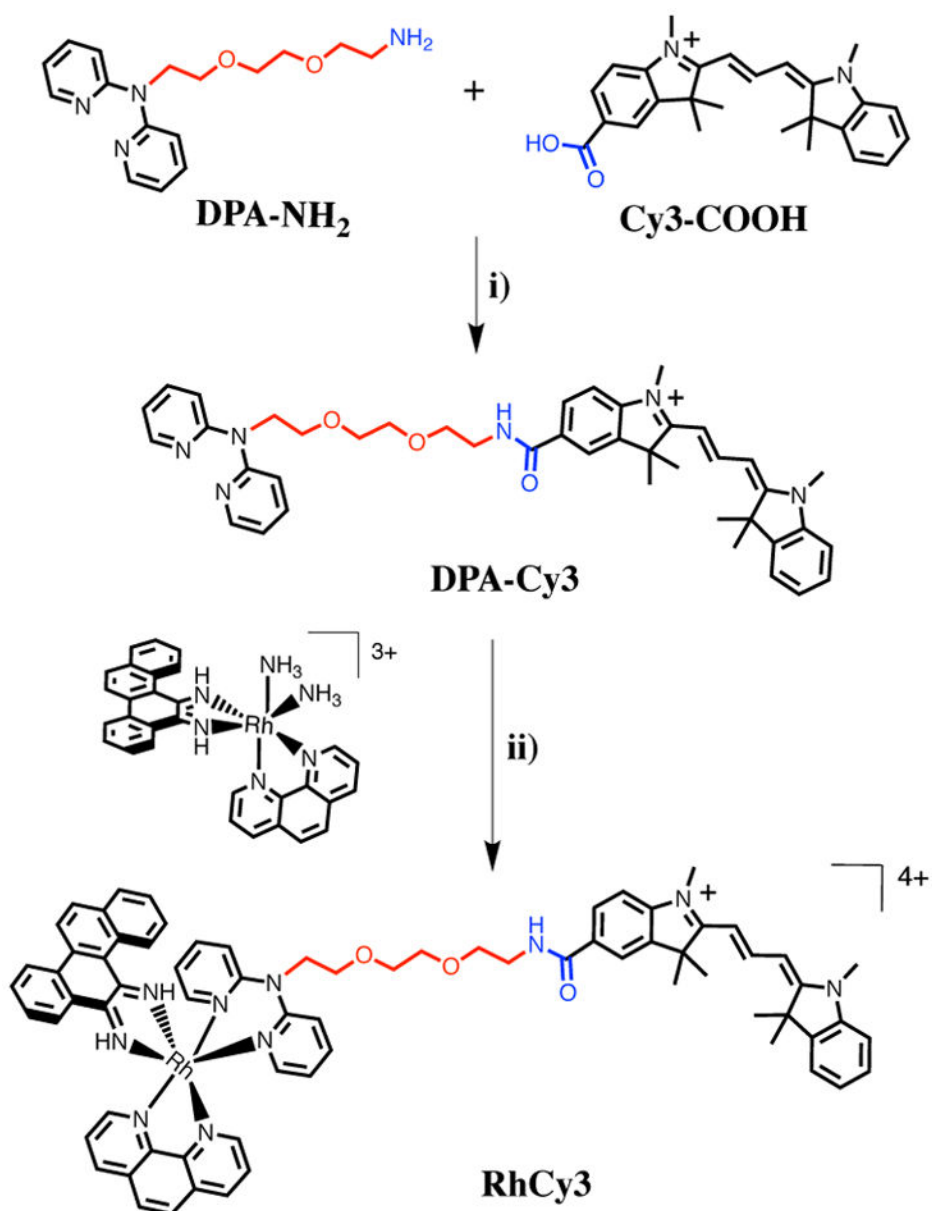


Figure 5. **RhCy3** fluorescence titrations with increasing amounts of gDNA extracted from HCT116N, HCT116O, SKOV3 and DU145 cell lines. The fluorescence was measured in Tris buffer at 25 °C. $\lambda_{\text{Ex}} = 520 \text{ nm}$. $[\text{RhCy3}] = 1 \mu\text{M}$. Error bars were calculated over two replicates. [gDNA] is per base pairs.

**Scheme 1.**

Synthetic strategy for **RhCy3**. i) HBTU, DIPEA, DMF 0°C, 1.5–2 hrs., 86% yield. ii) CH₃CN/H₂O/EtOH, 95 °C, overnight, then anion exchange with MgCl₂, 40% yield.

Table 1Excited state lifetimes (τ) of RhCy3 with WM and MM DNA (1:1 ratio) or without DNA.

Compound		τ_1 , ps ^a	τ_2 , ps
RhCy3	No DNA	111	-
	WM DNA	116	1,340
		(96%) ^b	(4%)
	MM DNA	91	308
(85%) ^b		(15%)	

^aErrors \pm 5%. Measurements were carried out in Tris buffer (aerated) using 1 μ M Rh and oligomers.

^bIn the presence of WM or MM DNA, two lifetimes were obtained resulting from a biexponential decay function. Percentages reflect the relative contributions of each lifetime component to the overall decay.